行政院國家科學委員會補助專題研究計畫 ˇ成果報告 期中進度報告

昆蟲腦部共軛焦顯微鏡影像分析之研究（2/2）

Research on confocal microscopic images of insect brain

計畫類別：☑ 個別型計畫　　□ 整合型計畫
計畫編號：NSC　91－2213－E－009－076－
執行期間：　91 年　8　月　1　日至　92　年　7　月　31　日

計畫主持人：荊宇泰
共同主持人：江安世,莊榮宏,謝昌煥
計畫參與人員：

成果報告類型(依經費核定清單規定繳交)：□精簡報告　☑完整報告

本成果報告包括以下應繳交之附件：
□赴國外出差或研習心得報告一份
□赴大陸地區出差或研習心得報告一份
□出席國際學術會議心得報告及發表之論文各一份
□國際合作研究計畫國外研究報告書一份

處理方式：除產學合作研究計畫、提升產業技術及人才培育研究計畫、列管計畫及下列情形者外，得立即公開查詢
□涉及專利或其他智慧財產權，□一年□二年後可公開查詢

執行單位：國立交通大學 資訊科學系

中　華　民　國　93　年　2　月　1 日

中文摘要

本計畫發展昆蟲腦共軛焦顯微鏡影像影像分析. 主要發展影像切割以及視覺化的演算法以及工具. 在本報告中我們提出切割 mushroom body 的方法, 神經纖維視覺化的方法, 神經追蹤演算法, 以及 bouton 的切割方法.

關鍵詞:共軛焦顯微鏡, 神經叢視覺化, 神經影像切割.

英文摘要

We studied the algorithms and methods for the analysis of the confocal microscopic images of a insect brain. In this report, we present some results obtained. The first is an algorithm to segment the mushroom body. The second is an algorithm for visualization of the neuron fibers. The other two algorithms are to segment the neuron fibers and the bouton on the neuron fibers.

Keywords: confocal microscopy, insect brain, neuron fiber visualization, neuron fiber segmentation.

一、計畫緣起及目的

Confocal microscopy reaches the best resolution that an optical microscopy can do. Other than the resolution, the confocal microscopy can produce a set of volume data of an object without actually section the object. With a proper staining technique, the confocal microscopy is the best tool to observe a single neuron or a set of neural fibers. Together with volume rendering technique, scientist can directly observe the relative position between a set of neurons.

There are two ways to generate 3D images for a set of neurons. The first is to apply the volume rendering technique, for example the ray casting or the marching cube technique. In this case, one has to define a mapping between the intensity of voxels in the image to the opacity used in the rendering process. The easiest one is to define a threshold for the isosurface. This strategy encounters a problem that the neuron fibers do not have a constant intensity for its surface. A proper preprocess step is required to enhance the neuron fibers in this case.

The other approach is to segment the neuron fibers directly. There were not many previous works to segment neuron fibers. Similar works were the segmentation of the blood vessel in angiogram. Segmentation of the neuron fibers is a much difficult task since neuron fibers are thing, and do not have constant intensity as mentioned previously. In this report, we present a neuron tracing algorithm to segment a single neuron fiber.

Bouton is a enlarged portion on the neuron fiber. The size of the bouton could represent important information in neural science. Since there are many boutons in on a set of neuron fibers, automatic method to segment the bouton is desired. In this report, we present a method to segment the bouton.

二、研究成果

Our results are listed in the following.

1. **Segmentation of the Mushroom body in an insect brain:** Landmark such as the mushroom body in an insect brain is important in research of the neural science. To segment the mushroom body, we propose a method developed

based on the GVF (Gradient Vector Flow) snake. First of all, we need an edge map to compute the GVF snake. The edge map is obtained by first computing the texture of the insect brain. A rough boundary is then obtained by texture analysis. The vector field is then obtained from the edge map. A snake is then converged under the guidance of the vector field. In this work, we also present a method to determine whether the snake reaches its steady state. The results are shown in Figure 1. The details can be found in an attached manuscript submitted for publication.

2. **Visualization of neuron fibers in an insect brain**: Neuron fibers are generally thing and hard to segmented. One way to visualize the fibers is to use the volume rendering technique to create a 3D image from the volume data. Unfortunately, the threshold for volume rendering is hard to define since neuron fibers do not have a constant intensity. To this problem, we proposed to enhance the neuron fibers before applying the volume rendering algorithm. The data studied was a set of two channels volume data. Two channels contain two sets of neuron fibers but have similar background. The first enhancement method was to apply wavelet transform to each channel. Since the neuron fibers are in the high frequency component and the common backgrounds are in the low frequency component, we subtract the low frequency wavelet coefficients but enhance the high frequency wavelet coefficients. We restored the images from the processed wavelet coefficients. Volume rendering algorithm is then applied the resulted image. The second approach was to employ the matched filter. Neuron fibers are tubular structure so that matched filter can enhance the fibers. Thus we applied multi-orientation-multi-width matched filter before the volume rendering we applied. The results are shown in the Figure 2. The details can be found in the attached manuscript published in SPIE MI2003.

3. **Segmentation of a neuron fiber**: Due to improvement of the staining skill, it is possible to have very few amount of neurons shown in the image. In this case, segmentation of a single neuron becomes possible. We developed a neuron tracing algorithm. User has to define an initial point and a direction that neuron grows. Our proposed method calculates the direction a neuron should grow based on the assumption-there are at most two branches at one point. The calculation used a matched filter to determine the largest response to determine the direction where a neuron grows. A part of the traced neuron is shown in Figure 3.

4. **Segmentation of bouton**: Bouton is a part of the neuron fiber that has a much larger width. Generally speaking, the number of boutons is not small. Our goal is to segment the boutons, count the number and the sizes of the bouton. And record the location of the bouton. We have developed a method based on computational geometry and graph

algorithm to segment the boutons. We briefly state the algorithm. The proposed algorithm needs an initial guess of the boundaries of the boutons. This can be achieved by intensity thresholding followed by connected component analysis. For each connected component, we can determine a rough boundary of the bouton. By growing the boundary points, we are able to determine a region, which is a band, that sandwitches the true boundary. The band has two closed contours that one encloses the other. The region in between these pair of closed contours is then triangulated by using the constrained Delaunay Triangulation. Finally, a weighted directed graph is established based on the Delaunay Triangulation. The boundary is then obtained by finding the shortest path of the graph. The results are shown in Figure 4. This method has been applied to segment other images such as echocardiogram, computed radiogram. In most of the cases, it achieves very good result. We believe it is a robust and general segmentation algorithm.

三、計畫成果自評

The result stated in the first part, segmentation of mushroom body, has been submitted to publication. The neuron fiber visualization work was published in the SPIE Medical Imaging 2003 which was held 2003 February in San Diego, California. The other two results were in the status of the refinement and preparation for possible publication. These developed can be applied to analysis of the neuron structure of the insect brain. We are confident on our results obtained from this project.

At the end of these report, we attaches two manuscripts. The first manuscript presents the algorithm to segment the neuropils in the confocal microscopic images. The second manuscript is the visualization of the neuron fibers work which has been published in SPIE Medical Imaging conference. Some of the details can be found in these manuscript.

參考文獻

1. Eric J. Stollnitz, Tony D. DeRose, and David H. Salesin, “Wavelets for Computer Graphics. Theory and Applications” Morgan Kaufmann Publishers, Inc., 1996.
2. Unser, Michael,1996.”Wavelets, statistics, and biomedical applications,” *8th IEEE Signal Processing Workshop on Statistical Signal and Array Processing*, Jun 1996 pp.: 244 -249
3. Anca Dima, Michale Scholz, and Klaus Obermayer, 2002. “Automatic Segmentation and Skeletonization of Neurons From Confocal Microscopy Images Based on the 3-D Wavelet Transform,” *IEEE Transactions on Image Processing*, July, Vol. 11, NO. 7, pp. 790-801
4. Chih-Yang Lin, Yu-Tai Ching, S. James Chen, “Extraction of Coronary Arterial Tree Using Cine X-Ray Angiograms”
5. Khalid A. Al-Kofahi, Sharie Lasek, Donald H. Szarowski, Christopher J. Pace, and George Nagy, 2002. “Rapid Automated Three-Dimensional Tracing of Neurons From Confocal Image Stacks,” IEEE Transactions on Information Technology in Biomedicine, June, Vol. 6, No. 2, pp. 171-187.
6. Chatterjee, S.; Chaudhuri, S.; Goldbaum, M.; Katz, N.; Nelson, M., 1989,”Detection of blood vessels in retinal images using two-dimensional matched filters,” *IEEE Transactions on Medical*

Imaging, Volume: 8 Issue: 3 , Sep 1989, pp. 263 -269

7. Goldbaum, M.; Hoover, A.D.; Kouznetsova, V., 2000, "Locating blood vessels in retinal images by piecewise threshold probing of a matched filter response," *IEEE Transactions on Medical Imaging,* Vol.: 19 Issue: 3 , Mar 2000, pp. 203 -210
8. S. Mallat, "A Theory fro Multiresolution Signal Decomposition: The Wavelet Representation," IEEE Trans.PAMI, vol. 11, pp. 647-693, 1999.
9. P. P. Vaidyanathan, "Multirate Systems And Filter Banks", Prentice Hall, Inc., 1993.
10. L. Cohen, "Time-Frequency Distributions - A Review," Proc. IEEE, Vol. 77, pp. 941-981, 1989

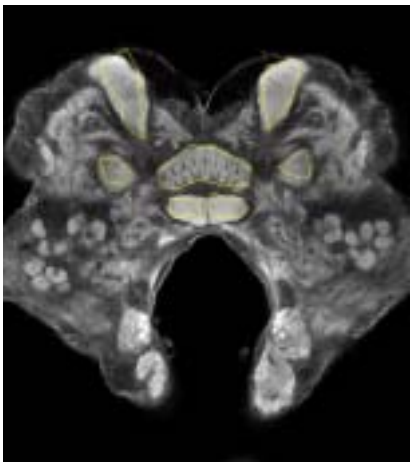

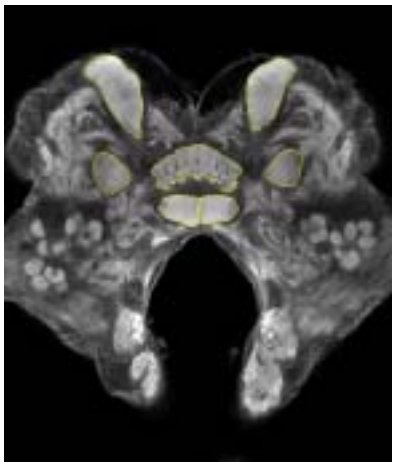

Figure 1. Segmentation of the mushroom body. The above one shows the initial snakes and the converged is shown in the below.

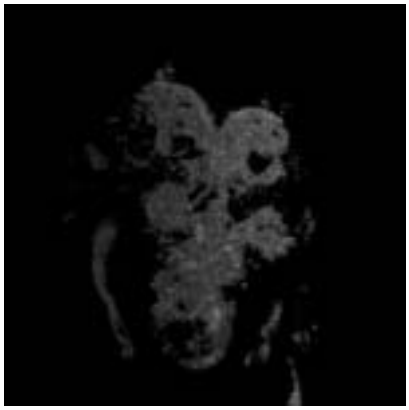

(a) without preprocessing

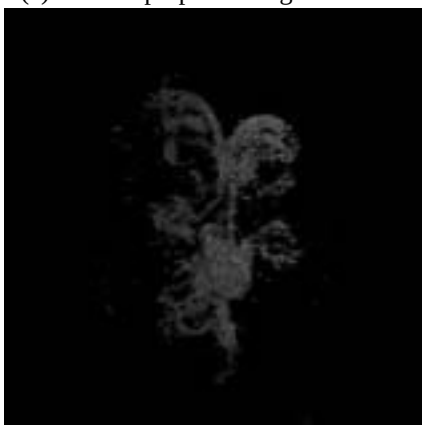

(b) preprocessed by Wavelet transform

(c) preprocessed by matched filter

Figure 2. Volume rendering of neuron fibers, (a) without preprocessing, (b) preprocess by using the wavelet transform, (c) preprocess by using the matched filter.

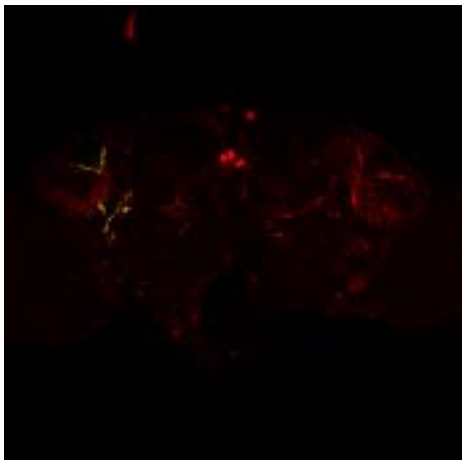

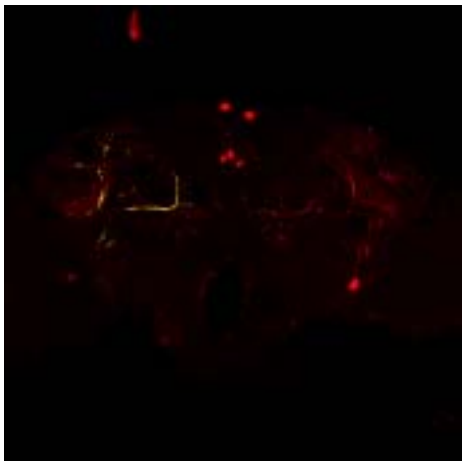

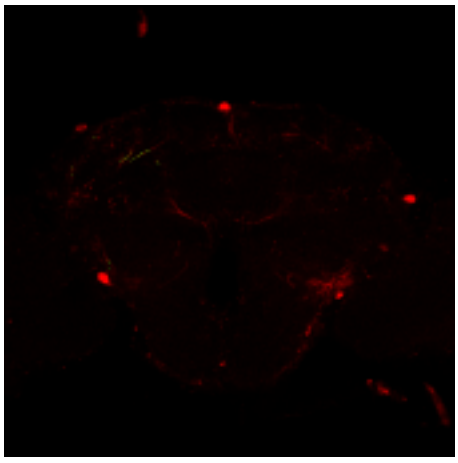

Figure 3. The results after neuron tracing by the proposed algorithm.

Figure 4. The bouton segmentation results.

Segmentation of Insect Brain Neuropils in the Confocal Microscopic Images Using GVF Snake[1]

Yu-Tai Ching[2], Chiy-Yang Lin, Min-Jin Wu
Department of Computer and Information Science
National Chiao Tung University
Hsin Chu, Taiwan 300

Ann-Shyn Chiang
Department of Life Science
National Tsing Hua University
Hsin Chu, Taiwan 300

Chang-Huain Hsieh
National Center for High Performance Computing Center
Hsin Chu, Taiwan 300

ABSTRACT

Volumetric analysis and 3D visualization of brain structures is valuable to neuroscience research. In this article, we use the Gradient Vector Flow (GVF) snake to segment mushroom body in an insect brain confocal microscopic image. The GVF snake has advantage of capturing local cavity. This also means that the GVF snake is sensitive to noises and needs good edge map. We employed the texture analysis and Canny edge detector to calculate a good edge map before the GVF was calculated. In this article, a new method based on global shape of a snake to define a halting condition from moving a snake is presented.

Keywords: active contour, snake, gradient vector flow, segmentation, confocal microscopic image, chain code encoding.

---

[1] This work was support under the grant NSC-91-2213-E-009-076, National Science Council, Taiwan.
[2] Correspondence please send to Yu-Tai Ching, Department of Computer and Information Science, National Chiao-Tung University, 1001 Ta-Hsueh Rd., Hsin Chu, Taiwan 300, email ytching@cis.nctu.edu.tw, Fax +886-3-572-1490, Phone +886-3-5131547.

Segmentation of Insect Brain Neuropils in the Confocal Microscopic Images Using GVF Snake

Yu-Tai Ching, Chiy-Yang Lin, Min-Jin Wu
Department of Computer and Information Science
National Chiao Tung University
Hsin Chu, Taiwan 300

Ann-Shyn Chiang
Department of Life Science
National Tsing Hua University
Hsin Chu, Taiwan 300

Chang-Huain Hsieh
National Center for High Performance Computing Center
Hsin Chu, Taiwan 300

ABSTRACT

Volumetric analysis and 3D visualization of brain structures is valuable to neuroscience research. In this article, we use the Gradient Vector Flow (GVF) snake to segment mushroom body in an insect brain confocal microscopic image. The GVF snake has advantage of capturing local cavity. This also means that the GVF snake is sensitive to noises and needs good edge map. We employed the texture analysis and Canny edge detector to calculate a good edge map before the GVF was calculated. In this article, a new method based on global shape of a snake to define a halting condition from moving a snake is presented.

Keywords: active contour, snake, gradient vector flow, segmentation, confocal microscopic image, chain code encoding.

1. INTRODUCTION

Confocal microscopy is widely used in neuroscience research because of its unique features in removing out-of-focus signals and volume visualization. This tool is particularly useful in studying brain neural networks projecting to a large space. Using the newly developed FocusClear^{TM} reagent to clear biological tissues together with confocal microscopy, it is now possible to image the whole insect brain of 500 micron thick without physical sectioning [1]. Mushroom bodies are neuropil regions in the insect brain that have been implicated in associative

learning and memory. Recently, a standard *Drosophila* brain averaging from several individuals has been established for comparing brain volumes between different wild types and mutants [2]. The so-called standard brain provides a common 3D framework as the first step for building a brain database allowing deposition of gene expression patterns from different laboratories. Consequently, averaged neuropils for detail analysis of brain's function are urgently needed. Automatic segmentation of neuropils is the one of the most fundamental task to establish averaged neuropils.

In this article, we present an almost automatic method to segment the mushroom body in a stack of confocal microscopic volume images of cockroach brain. Difficulty in this task is mostly due to the vague boundary between the mushroom body and the background. The traditional low-level techniques such as intensity thresholding or gradient based edge detecting methods which only utilize local information could make mistakes during creating the boundary. To overcome this problem, the active contour model, known as "snake", which has been introduced by Kass, Witkin and Terzopoulos in 1987 [3], integrates the image feature extraction and representation phase into a single process. A snake is an energy-minimizing curve defined within an image domain that moves under the influences of the internal forces coming from within the curve itself and the external forces computed from image data. The internal and external forces are defined such that the snake will be attracted to an object boundary or other features within an image. Snakes are widely used in many applications, including edge detection [3], shape modeling [4], segmentation [5], and motion tracking [6]. In this study, we adopted the active contour model using the gradient vector flow (GVF) [7] as the external force to segment the mushroom body in the cockroach brain image.

As mentioned previously, the major difficulty to segment the mushroom body is due to the vague boundary between the mushroom body and the background. Vague boundary implies weak external force to attract the snake. To enhance the boundary of the mushroom body, we proposed to first apply the texture analysis to the image. We then applied the Canny edge detection method to calculate the boundary between the mushroom body and background. The gradient vector flow is finally calculated using the edge map obtained from the Canny edge detector. In the next section, we first state the proposed method. We then briefly describe the techniques involved in

each step of the method. We also present a new halting condition to test if the snake converged. In Section 3, we demonstrate the result obtained using the proposed method. The conclusions are in Section 4.

2. METHOD

In this section, we first outline each step in the proposed method. We then describe the methods employed in each step.

The outline of the steps is stated in the following.

1. Texture analysis: Since the mushroom body has different texture from the background, image after texture analysis enhances the mushroom body as well as the boundary between the mushroom body and the background. The mushroom body in the image after texture analysis has low intensity in the image. Thus, the intensity thresholding can then be applied to segment the mushroom body.

2. Edge detection: Canny edge detection algorithm is then applied. The edges of the mushroom body have strong response. Applying the intensity thresholding can eliminate most of the noises. The resulted image is the edge map.

3. Calculate the GVF based on the edge map obtained.

4. Applied the active contour method to segment the mushroom body.

2.1 Texture Analysis

Texture analysis helps to divide an image into regions according to the textures of the regions. There are many ways to define the texture in a region. One of the ways is the "coefficient of variance", *CV*, that is defined as the following equation.

$$CV = \frac{\sqrt{\sigma}}{\mu}. \qquad (1)$$

In Eq. (1),

$$\mu = \frac{\sum_{k=1}^{N} f(k)}{N}, \text{ and}$$

$$\sigma = \frac{\sum_{k=1}^{N} f(k) - \mu}{N}.$$

Note that, a large *CV* means large deviation in the a region *f*(*k*). On the other hand, a region has small *CV* implies that the region *f*(*x*) has uniform distributed intensity. In our application, the mushroom body has small deviation of the intensity than the background, thus the coefficient of variance analysis produces small *CV* in the mushroom body.

2.2 Canny Edge Algorithm

Canny edge algorithm was proposed by Canny in 1986 [8]. Three issues regarding an edge detector were addressed:

1. Correct Detection: The truth positive and the truth negative ratio should be high. And the false positive and the false negative ratio should also be high.
2. Good Localization: Points detected by the operator should be as close to the real edge as possible.
3. Good Response: Only one response to a single edge. If too many edges are detected, then obviously some of them must be false edges.

Based on the addressed issues, designing an optimal filter was modeled as an optimization problem. Since the optimal solution was difficult to solve, Canny used an approximation method to design a filter that is close to the optimal filter. The function is the derivative of a Gaussian as shown in Eq. (2).

$$g'(x) = -\frac{x}{\sigma^2} e^{-x^2/2\sigma^2} \qquad (2)$$

The next step in the Canny edge detector is to find thin edges by using a “non-maximum suppression” technique. In this step, pixels that are not local maximal are removed. The last step is the hysteresis thresholding. Hysteresis thresholding sets a high threshold T_h and a low threshold T_l. Any pixel in the image that has a value greater than T_h is presumed to be an edge pixel. Then

any pixel, that is connected to an edge pixel and has a value grater than T_l , is selected to be an edge pixel.

2.3 Active Contour Method and Gradient Vector Flow

An active contour model is a mapping: $\Omega = [0 , 1] \rightarrow R^2$, and $S \rightarrow v(s) = (x(s) , y(s))$. We define the model as a space of admissible deformation A and a function E to be minimized. This function E is written in the form

$$E = \int_0^1 E_{int}(v(s)) + E_{ext}(v(s))ds , \tag{3}$$

where E_{int} represents the internal energy of a snake due to bending, and E_{ext} the external force that is derived from image features. E_{int} serves to impose smoothness constraint on the snake. E_{ext} pushes or pulls the snake toward desired features such as edges. As internal and external energy are formulated, we deform the snake by minimizing Eq. (3). The internal energy can be written as:

$$E_{\text{int}} = (\alpha(s)\left|v'(s)\right|^2 + \beta(s)\left|v''(s)\right|^2)/2 \tag{4}$$

where $\alpha(s)$ and $\beta(s)$ are weighting parameters that control the snake's elasticity and rigidity, $v'(s)$ and $v''(s)$ denote the first and second derivatives of the curve v with respect to s. The energy function that attracts snake to salient features in images is the external energy. External energy is derived from the image.

Traditional active contour model suffers from the following three key difficulties: First, the active contour model has narrow capture range. Second, active contour model lacks the ability to handle boundary concavities. Third, snake has the tendency to become stagnant at a nearby local energy minimum. For the third problem, the main difficulty is due to noise. Preprocessing of the image is necessary. Texture analysis mentioned previously is employed to reduce noise. However, if the noise is too strong, it still requires user assists to manually adjust the snake to escape from the local minimum. For the first and second problem, Xu and Prince proposed a method called the Gradient Vector Flow (GVF) in 1998 [7] to solve the problems.

The GVF field is defined to be a vector field $p(x,y) = [g(x,y),h(x,y)]$ that minimize the energy

$$\xi = \iint \mu(g_x^2 + g_y^2 + h_x^2 + h_y^2) + |\nabla f|^2 |p - \nabla f|^2 \, dxdy \,. \tag{5}$$

When $|\bigtriangledown f|$ is small, the energy is dominated by the sum of the squares of the partial derivatives of the vector field, yielding a slowly varying field. On the other hand, when $|\bigtriangledown f|$ is large, the second term dominates the integrand, and is minimized by setting $p = \bigtriangledown f$. This produces the desired effect of keeping p nearly equal to the gradient of the edge map when it is large, but forcing the field to be slowly-varying in homogeneous regions. Using calculus of variations [9], it can be shown that the GVF field can be found by solving the following Euler equations:

$$\mu \nabla^2 g - (g - f_x)(f_x^2 + f_y^2) = 0 \text{, and} \tag{6a}$$

$$\mu \nabla^2 h - (h - f_x)(f_x^2 + f_y^2) = 0 \,, \tag{6b}$$

where $\bigtriangledown^2$ is the Laplacian operator.

Using GVF to server as external forces, we can move the snake to minimize the energy of the contour shown in Eq. (3). The solution can be solved by using the greedy approach [10] or the finite difference method [3]. We used the finite difference method in our implementation.

2.4 Implementation Details

Two issues are discussed in this section, the reparameterization of a contour and the halting condition of a moving snake.

When a snake deforms, the distances between consecutive vertices on the snake change. It is required to resample the snake along its path [11]. We resample the snake according to a user pre-defined parameter l_{des}. The distance between the neighboring vertices is kept between $0.5l_{\text{des}}$ and $1.5l_{\text{des}}$. When the distance is less than $0.5l_{\text{des}}$, we merge two adjacent vertices into a single vertex. If the distance is larger than $1.5l_{\text{des}}$, we insert a vertex between the vertices.

The next issue is the halting condition for a snake. One possible condition is to set a limit for the number of iterations. Another approach is to monitor the improvement (change of energy)

between two consecutive iterations. The snake stops moving if the improvement is small enough. Due to the following reason, we present a new method to determine the halting condition.

Since the external force is provided by the GVF, the vertices on the snake move toward "valley" of the external force field when a snake converges. Since the bottom of the valley is not at the same height, some points in the valley still move toward nearby local minimal even when the snake converge to the boundary. In such cases, in order to reduce the energy of the snake, vertices of a snake will have a strong tendency to pile up in the "deepest pocket" in the valley. To solve this problem, we define the stopping criterion as the similarity of the shapes of contours. If the similarity between two snakes is within a threshold, we consider these two snakes to be the same and confirm that the snake is converged. To evaluate the similarity of the shapes of contours, we adopt a modified chain code curve encoding method [12] and the longest common subsequence techniques[13].

Chain code encoding method is first proposed by Freeman [12]. The concept is to divide a curve into a fixed length segment and encode the curve according to the direction of segments along the curve. In general, encoding method has 4-connectivity (Fig. 1) and 8-connectivity (Fig. 2). We subdivide the plane into 4 (8 respectively) regions in 4-connectivity (8-connectivity respectively) for encoding. Given a starting vertex on a curve, we compute the vector of adjacent vertices along the curve. Then we encode the curve into a bit string according to the directions of the vectors. We call the bit in a bit-string as *direction bit*. Fig. 3 shows an example in a 8-connectivity encoding of a curve.

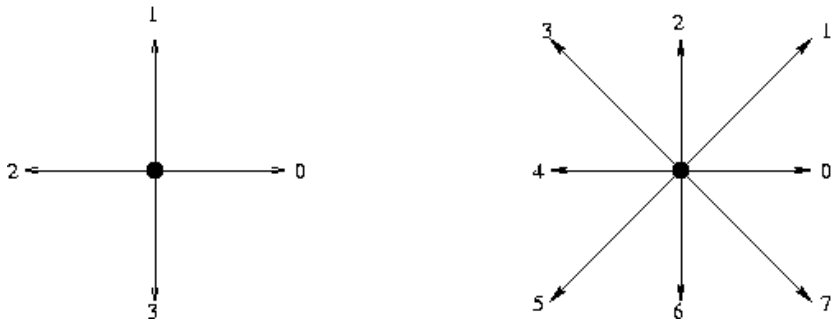

Fig. 1 4-connectivity and 8-connectivity for chain code encoding

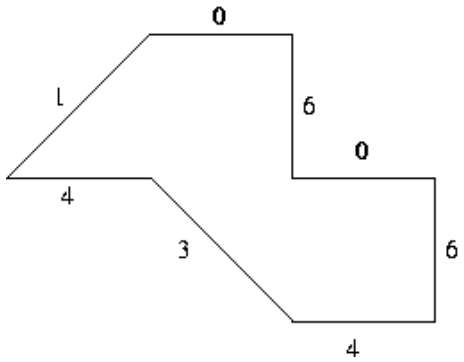

Fig. 2 An example of 8-connectivity chain code encoding in clockwise order

When two curves are encoded into two bit-strings, we find the longest common subsequence (LCS) of these strings by the dynamic programming technique [13]. We define a similarity function as follows:

$$S(v1, v2) = (Len(v1) + Len(v2) - 2 \times LCS(v1, v2)) / (Len(v1) + Len(v2)). \quad (7)$$

In Eq. (7), S denotes the similarity function. $v1$ and $v2$ are curves to be matched. $Len(v)$ denotes the length of the curve v, and $LCS(v1, v2)$ denotes the length of the longest common subsequence of $v1$ and $v2$. Note that $0 \le S(v1, v2) \le 1$. If two curves are identical, $S(v1, v2) = 0$. A small S implies two curves are identical. We set a threshold T_s that if S is smaller than T_s, we consider that the snake has been converged.

A standard chain code has a problem. In figure 4, vector **A** and vector **B** are in different encoding regions. Thus vector **A** and **B** is considered pointing in different direction and are encoded into distinct direction bits. But if the angle in vector **A** and **B** is small, they should be considered pointing in the same direction. Thus, we made a modification in defining the cost function in the longest common subsequence algorithm to solve this problem. In the original longest common subsequence algorithm, a string bit represents vector ' s direction. Now we let each string bit to be the vector itself. The comparison of string bits is replaced by the inner product of the vectors. If the value of the inner product is larger than a given threshold value θ, we consider these two string bits are identical. According to our experiment, the modified method provides a reliable stopping criterion.

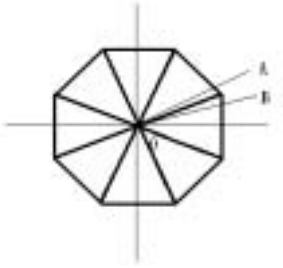

Fig. 3 Vector **A** and **B** are similar. But they are considered very different in chain code encoding.

2.5 User Interface

Snakes can be trapped into local minimal or wrongly converged to a boundary due to noises or ill initialization. When this happens, user assist is used to help the snake to escape from the trapped configuration. The other situation that needs a user assist occurs when the topology of contour changes. When a contour splits into two contours or two contours merge into one contour, we need user assists to manually modify the snakes.

3. EXPERIMENTAL RESULT

We present the experimental results by using two images. The first image is shown in Fig. 4. In this figure, the original image is in (a). In (b), the image after texture analysis is shown. (c) shows the image after intensity thresholding of the image (b). Images (d) and (e) are obtained by first applying the Canny edge detector and the intensity thresholding of the image after Canny edge detection. The initial contour is shown in (f). (g) is the image consists of the initial contour and the calculated GVF. Images in (h) and (i) are the converged snakes for both the left and right mushroom bodies. The converged snakes for the mushroom bodies superimposed in the original images are shown in (j) and (k). The second image has worse contrast than the previous one. We show that the proposed method can still segment the mushroom body well. In the first row in Fig. 5, there are the original image, the image after texture analysis, and the image after intensity thresholding of the resulted image after texture analysis. The second row consists of the images that are obtained by the Canny edge detection, intensity

thresholding of the resulted image after Canny edge detection, and the calculated GVF as well as the initial contour. In the third row, there are two images showing the converged snakes. Even the contrast is much worse than the previous image, the proposed method can still well segment the mushroom body.

4. DISCUSSION

We presented a method to segment the mushroom body in the confocal microscopic image. The proposed method employed the texture analysis and the Canny edge detector method to compute the edge map. The active contour method using GVF as the external force was then used to segment the mushroom body. The proposed method worked well even when the boundary of the mushroom body is not very sharp.

When we apply the method to segment the 3D mushroom body in a stack of volume images, the final converged contour in one slice serves as the initial contour in the next slice. The user assists are needed when the topology of the contour changes or there are unexpected noises. This method helps to reduce the required of human intervene to process a whole stack of volume data.

The disadvantage of this approach is the computing time required in the preprocess step. To compute the GVF of a 256 by 256 image needs 5 seconds in an AMD 1.5G XP CPU PC. However, since it generally takes less than an hour to process a set of volume data, and it does not need any human intervene in the preprocessing step, the proposed method can save many man power in the task of segmentation of the mushroom body.

REFERENCES

1. Chiang AS., Liu YC., Chiu SL., Hu SH, Huang CY, and Hsieh CH. (2001) Three-dimensional mapping of brain neuropils in the cockroach, *Diploptera punctata*. J. Comp. Neurol. 440, 1-11.
2. Rein K, Zockler M, Mader MT, Grubel C, and Heisenberg M. (2002) The *Drosophila* standard brain. Curr. Biol. 12, 227-231.

3. M. Kass, A. Witkin, and D.Terzopoulos, “Snakes: Active contour models,” *Int. J. Comput. Vis*., vol. 1, pp.321-331, 1987.
4. D. Terzopoulos and K. Fleischer, “Deformable models,” *Vis. Comput*., vol. 4, pp. 306-331, 1988.
5. F. Leymarie and M. D. Levine, “Tracking deformable objects in the plane using an active contour model,” *IEEE Trans. Pattern Anal. Machine Intell*., vol. 15, pp. 617-634, 1993.
6. D. Terzopoulos and R. Szeliski, “Tracking with Kalman snakes,” in *Active Vision*, A. Blake and A. Yuille, Eds. Cambrige, MA: MIT Press, 1992, pp. 3-20.
7. Chenyang Xu and Jerry L. Prince, “Snakes, Shapes, and Gradient Vector Flow,” *IEEE Transactions on Image Process*, vol. 7, no. 3, Mar. 1998.
8. J. Canny., “A computational approach to edge detection,” *IEEE Transactionis on Pattern Analysis and Machine Intelligence.*, Vol 8, pp670-698, 1986.
9. R. Courant and D. Hilbert, *Methods of Mathematical Physics*, vol. 1. New York: Interscience, 1953.
10. D.J. Willianms and M. Shuh, “A fast algorithm for active contours and curvature estimation”, *CVGIP:Image Understanding,* Vol. 55, No. 1, pp. 14-26, 1992.
11. S. Lobregt and M. A. Viergever, “A discrete dynamic contour model,” *IEEE Trans, Med. Imag*., vol. 14, pp. 12-24, Mar. 1995.
12. H. Freeman, “On the encoding of arbitrary geometric configuration,” *IRE Transactions on Electronic computers*, 1961.
13. T. H. Cormen, C. E. Leiserson and R. L. Rivest, *Introduction to Algorithms*. MIT Press, 1989.
14. A. H. Charles and T. A. Porsching, *Numerical Analysis of Partial Differential Equations*. Englewood Cliffs, NJ: Prentice-Hall, 1990, reading.
15. W. F. Ames, Numerical Methods for Partial Differential Equations, 3rd ed. New York: Academic, 1992, reading.

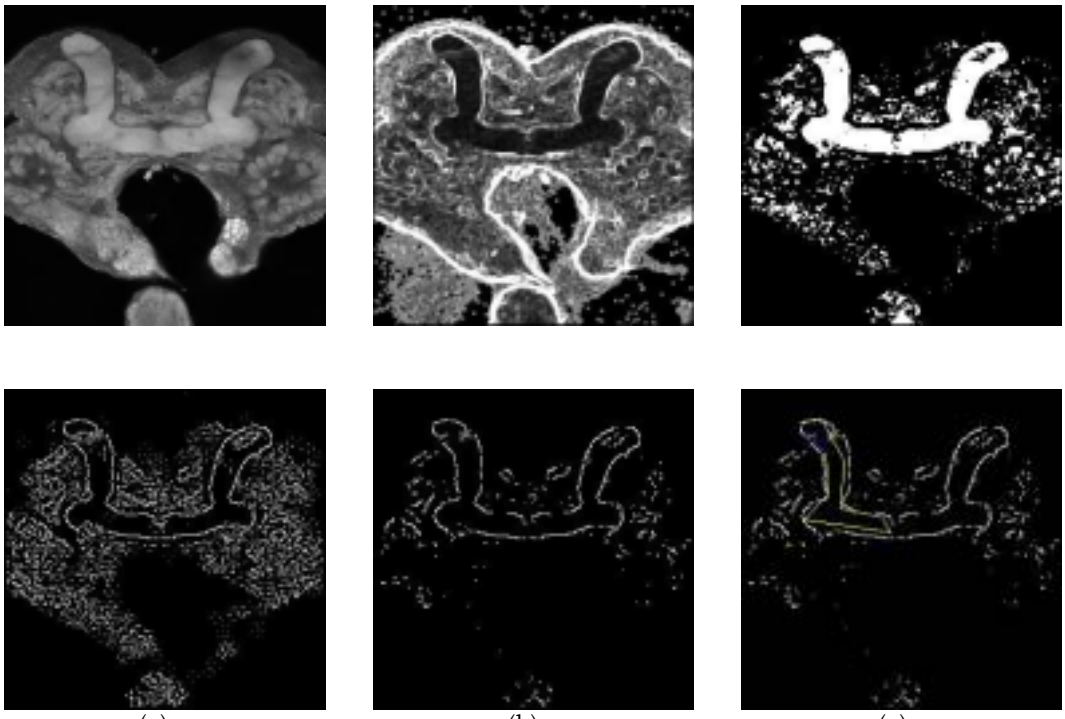

(a) (b) (c)

(d) (e) (f)

(g) (h) (i)

(j) (k)

Fig. 4 The first image. (a) is the original image. (b) and (c) The image after texture analysis and intensity thresholding. (d) and (e) show the images after Canny edge detector and intensity thresholding to obtain the edge map. (f) and (g) shows the initial contour. (h) and (i) are the converged snakes for the left and right mushroom body. In (j) and (k), we draw the contours on the original image.

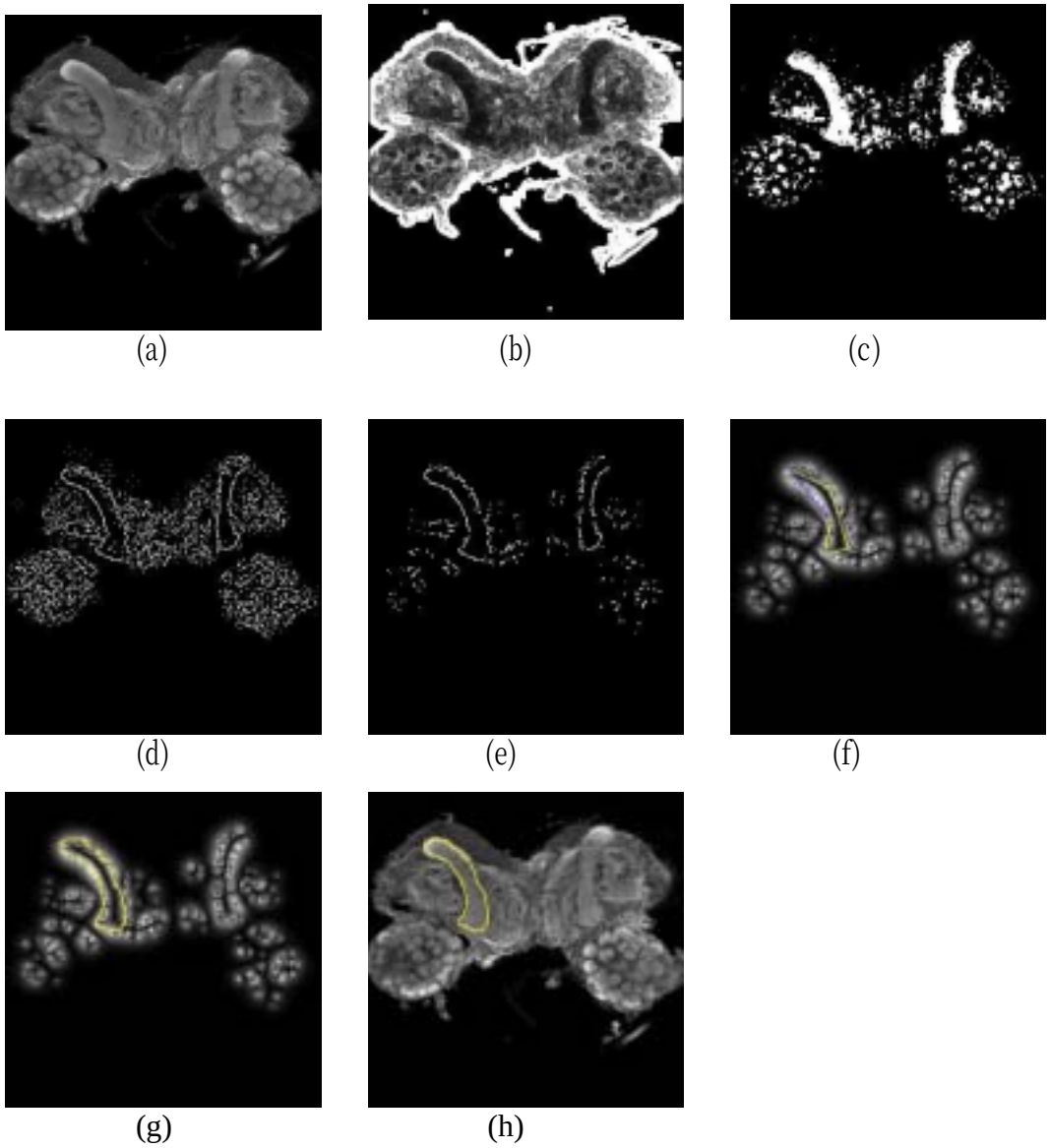

Fig. 5 The contrast of this image is worst than the one shown in Fig. 5. (a) The original image. (b) The image after texture analysis. (c) Intensity thresholding of the image after texture analysis. (d) and (e) are the images after Canny edge detector and intensity thresholding. (f) The initial contour. (g) The converge snake for one of the mushroom body. (h) is the converged contours drown over the original image.

Volume rendering the neural network in an insect brain in confocal microscopic volume images

Fu-Chi A. Ku and Yu-Tai Ching
Department of Computer and Information Science, National Chiao-Tong University, HsinChu, Taiwan, R.O.C
E-mail: alexku@cis.nctu.edu.tw, ytching@cis.nctu.edu.tw

1. ABSTRACT

Confocal microscopy is an important tool in neural science research. Using proper staining technique, the neural network can be visualized in the confocal microscopic images. It is a great help if neural scientists can directly visualize the 3D neural network. Volume render the neuron fibers is not easy since other objects such as neuropils are also polluted in the staining process and the neuron fiber is thin comparing to the background. Preprocessing of the image to enhance the neuron fibers before volume rendering can help to build a better 3D image of the neural network. In this study, we used the Fourier Transform, the Wavelet Transform, and the matched filter techniques to enhance the neural fibers before volume rendering is applied. Experimental results show that such preprocessing steps help to generate a more clear 3D images of the neural network.

Keywords: neuron fibers visualization, confocal microscopic volume image, Wavelet transform, matched filter, volume rendering.

2. INTRODUCTION

The brain has always been a interesting topic to researchers. It consists of millions of neurons and almost each of them has different functions. Studying the insect brains could help neural scientist to understand the human brains. Directly visualization of the neural network helps researcher to understand the possible interaction between neurons. In this study, we developed preprocessing methods to enhance the neuron fibers to help to get clear 3D images.

Confocal microscopy is a scanning laser technique that allows the recording of 3-D images of small objects usually stained with a fluorescent dye. During the scanning, each voxel is illuminated in turn by a focused laser beam. The photons emitted by the fluorescent dye are filtered by a small pinhole and the remaining photons are detected by a photomultiplier. There are several advantages of confocal microscopy. 1) It is a 3-D detector, by moving the laser header and modifying the intensity of laser beam, the inside voxel can also be illuminated. Therefore, the tissue deformations due to cutting can be avoided. 2) Signal-to-noise ratio is improved. 3) Blurring is reduced. 4) Axial resolution is considerably higher.

Although confocal microscope produces satisfied image than conventional ones, there are still works yet to be done in order to clearly visualize the 3D neural network. First of all, backgrounds still exist, and sometimes overlapped with our target objects. The second is the large variations in image contrast. This made it difficult on automatic thresholding. Third, the object size and intensity across different slices are usually different due to the anatomy position, and the neuron fiber stretches to a variety of directions. So the tracing on target object became a hard work. Due to the problems stated above, it is difficult to have an automatic method to preprocess the images. In this study, we introduce a semi-automatic method to handle the problems above. The presented method employs Fourier Transform, Wavelet Transform and the matched filter techniques.

Wavelet Transform [1][2] and Fourier Transform are widely used on noise reduction. Anca Dima et al. used a 3-D Wavelet Transform on confocal microscopy image [3]. Lin et al. also used it on the segmentation of coronary arteries [4] with matched filter. Khalid A. Al-Kofahi et al. used the neuron topology to extract the tree dimensional structure of a neuron cell [5]. In the conventional methods, a high (or low) pass filter is usually employed to filtrate out undesired signals. In this study, a different way of band information process is applied on the image, that different result is produced. Matched filter is also useful in medical image, especially on vessel detections [6][7]. In the former study, matched filter is applied to the segmentation of retinal vessels. Like vessel, neuron fibers are also tubular objects so that we use matched filter in our experiments to enhance the fiber.

The data studied is a set of brain images of cockroach. There are 38 slices of images. Each one has resolution 1024×1024. There are two channels in the data set. These two channels present different sets of neural network but have similar backgrounds.

In Section 2, the processing methods are introduced. Experiments and results will be put in Section 3. Finally, conclusion and summaries will be found in Section 4.

3. METHODS

3.1 WAVELET TRANSFORM

A standard Discrete Wavelet Transform (DWT) is summarized as follows and the details can be found in [8][9][10]. The DWT employs a pair of orthogonal high-pass and a low-pass filter to decompose an input signal into high frequency and low frequency components in different resolutions according to the number of levels employed as shown in Figure 1. In the one-dimensional (1-D) case, a signal $x(n)$ is decomposed iteratively by applying the low-pass and the high-pass filters as shown in Figure 1(a). Also a decomposed signal can be reconstruct from its DWT coefficients as shown in Figure 1(b).

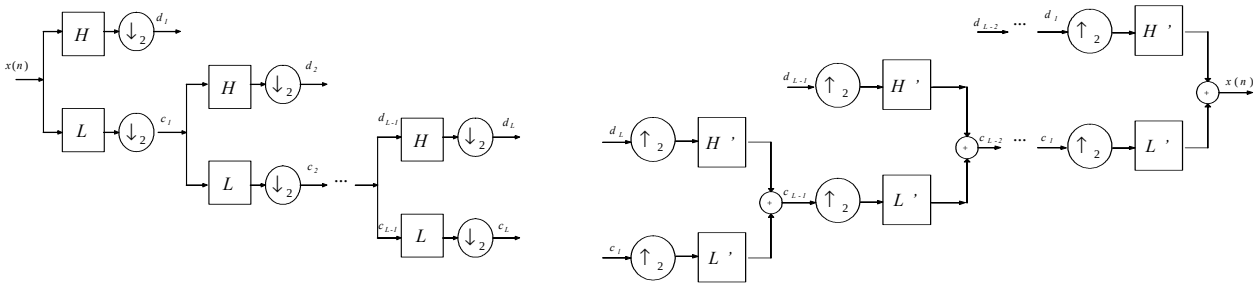

(a) (b)

Figure 1: Multi-level Wavelet (a) decomposition and (b) reconstruction for 1-D case

A two dimensional discrete Wavelet transform (2-D DWT) and its inverse are extended from the one-dimensional transform. It is implemented by applying one-dimensional DWT and IDWT along each of x and y coordinates. In other words, we apply a low-pass filter and a high-pass filter along each of the two coordinates. The original 2-D signal in the form of an image is then divided into four regions:

LL: obtained by applying two low-pass filters on both coordinates,

HL and *LH*: obtained by applying a high-pass filter on one coordinate and a low-pass filter on the other coordinate, and

HH: obtained by applying two high-pass filters on both coordinates.

The 2-D DWT, like the 1-D DWT, can be decomposed iteratively by using the pair of low-pass and the high-pass filters to establish a *k*-stage discrete Wavelet transform on the *LL* component

The first stage of the transform is to decompose the image into four equal size sub-images corresponding to the upper left (LL_1), the upper right (HL_1), the lower left (LH_1), and the low right (HH_1) regions. In the second stage, LL_1 is decomposed into four sub-images again. For the subsequent stage j, the upper left image (LL_{j-1}) is further decomposed to four sub-images. The typical example is illustrated in Figure 2.

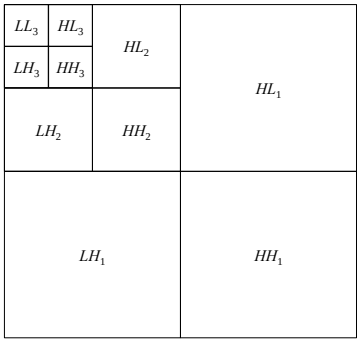

Figure 2: A 2-D 3-stage discrete Wavelet transformation

In the proposed method, we applied the Wavelet transform. Since the edge signals are in high frequency channels, we enhance the *HH*, *HL* and *LH* sub-image on each level. We then reconstruct the original image by using these enhanced sub-images (called *HH'*, *HL'* and *LH'*). The enhancement is shown in equation 1,2 and 3:

$$W(LL_i,\ LH_i,\ HL_i,\ HH_i) = DWT(LL_{i-1}) \quad for\ i \geqq 0,\ \text{where}\ LL_0 = f\ (x,y), \tag{1}$$

$$HH'_i = k \times HH_i \times k,\ HL'_i = k \times HL_i,\ LH'_i = k \times LH_i \qquad \text{where}\ k \in R, \tag{2}$$

$$LL'_{i-1} = IDWT(LL'_i,\ LH'_i,\ HL'_i,\ HH'_i)\ for\ i \geqq 0,\ \text{where}\ LL_0 = f'(x,y). \tag{3}$$

In the equations above, $f(x,y)$ and $f'(x,y)$ denote the original image and the result image. And i denotes the level of discrete Wavelet transform.

The second method needs two channels. Since there are two channels and these two channels have similar background, the second method based on the Wavelet transform takes advantage of this property to reduce the background. An averaged *LL* sub-image is produced simply by taking the average of the *LL* sub-image of the two channels of the same slice as shown in equations (4)-(7).

$$W_a(LL_{ai},\ LH_{ai},\ HL_{ai},\ HH_{ai}) = DWT(LL_{ai-1}) \quad for\ i \geqq 0,\ \text{where}\ LL_{a0} = f_a\ (x,y)$$

$$W_b(LL_{bi},\ LH_{bi},\ HL_{bi},\ HH_{bi}) = DWT(LL_{bi-1}) \quad for\ i \geqq 0,\ \text{where}\ LL_{b0} = f_b\ (x,y) \tag{4}$$

$$LL'_{ai} = LL'_{bi} = (LL_{ai} + LL_{bi}) \ / \ 2 \tag{5}$$

$$HH'_{ai} = k \times HH_{ai} \times k,\ HL'_{ai} = k \times HL_{ai},\ LH'_{ai} = k \times LH_{ai} \qquad \text{where}\ k \in R$$

$$HH'_{bi} = k \times HH_{bi} \times k,\ HL'_{bi} = k \times HL_{bi},\ LH'_{bi} = k \times LH_{bi} \qquad \text{where}\ k \in R \tag{6}$$

$$LL'_{ai-1} = IDWT(LL'_{ai},\ LH'_{ai},\ HL'_{ai},\ HH'_{ai})\ for\ i \geqq 0,\ \text{where}\ LL_{a0} = f'_a(x,y)$$

$$LL'_{bi-1} = IDWT(LL'_{bi},\ LH'_{bi},\ HL'_{bi},\ HH'_{bi})\ for\ i \geqq 0,\ \text{where}\ LL_{b0} = f'_b(x,y) \tag{7}$$

In the equations above, $f_a(x,y)$ and $f_b(x,y)$ denote the original image of channel a and channel b, $f'_a(x,y)$ and $f'_b(x,y)$ denote the resulted image of channel a and channel b, LL_a, LH_a, HL_a, HH_a, LL_b, LH_b, HL_b and *HHb* denote the *LL*, *LH*, *HL* and *HH* sub-image of channel a and channel b respectively. And i denotes the level of discrete Wavelet transform.

3.2 MATCHED FILTER

As mentioned previously, the neuron fibers are tubular objects, thus a rectangular matched filter is feasible for enhancing our image. Since matched filter is sensitive to noise, preprocessing of the image is necessary. In our

method, the Fourier Transform and the Wavelet Transform are employed to reduce the background and noise. Afterwards, the Gaussian distribution is introduced to generate this matched filter as shown in Equation (8).

$$g_1(x,y) = 1 - e^{-x^2/2\sigma^2} \tag{8}$$

The proposed matched filter is equipped with two parameters, the orientation θ and the size σ. An angular resolution of 15 ° was used in the implementation. Due to the various sizes of neuron fibers on thickness, different sizes of matched filters are necessary. In this study, the σ is set from 1 to 3, with a 0.5 increasing in each step. That is, 6 different sizes of matched filter is employed each angel. Each result will be convolved and the strongest response is retained.

4. EXPERIMENTAL RESULTS

4.1 RESULTS OF WAVELET TRANSFORM

In this section, the results produced by the proposed methods are presented. The data set being processed is a confocal microscopic volume image of cockroach brain with 38 slices of a resolution of 1024×1024. Each slice has two channels that come from different kind of dye. Figure 3 and Figure 4 shows the original image and the volume rendered results respectively. Since the between-pixel-distance on *x*, *y* and *z* axis are distinct (*x* : *y* : *z* = 1.12 : 1.12 : 4), so the resizing of the image is necessary. The new size of the image is 287×287×38. Volpack 1.0-b3, which is designed by Stanford University is employed as the volume rendering tool.

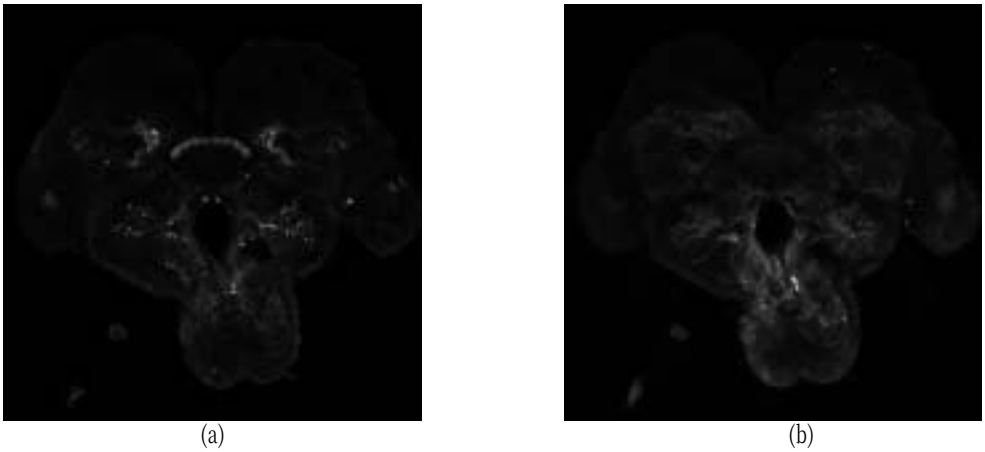

(a) (b)

Figure 3: slice 19 of the dataset (a) is the first channel (b) is the second channel

Observe that, the two channels have similar background. The second method of Wavelet transform can be applied. Figure 4 shows the volume rendering results obtained from the original, unprocessed image. The unwanted objects mixed with the desired neuron fibers after volume rendering. In Figure 5, the result of applying the first method of Wavelet transform is presented, and the second method of Wavelet transform is shown in Figure 6.

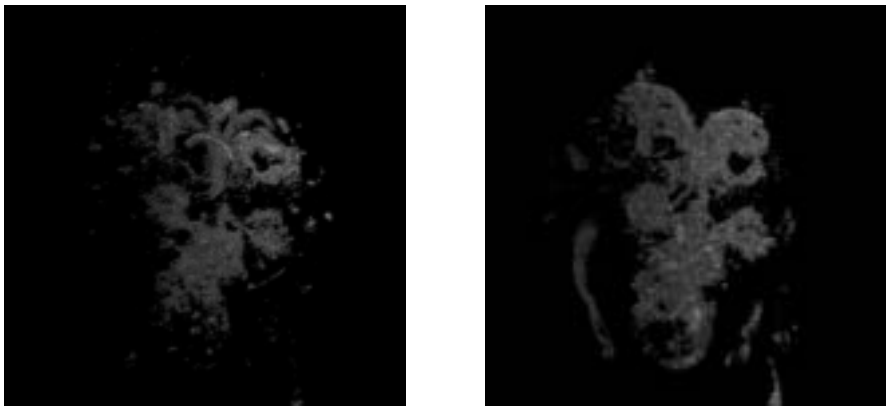

(a) (b)

Figure 4: the volume rendered image of the unprocessed image from (a) the first channel and (b) the second channel

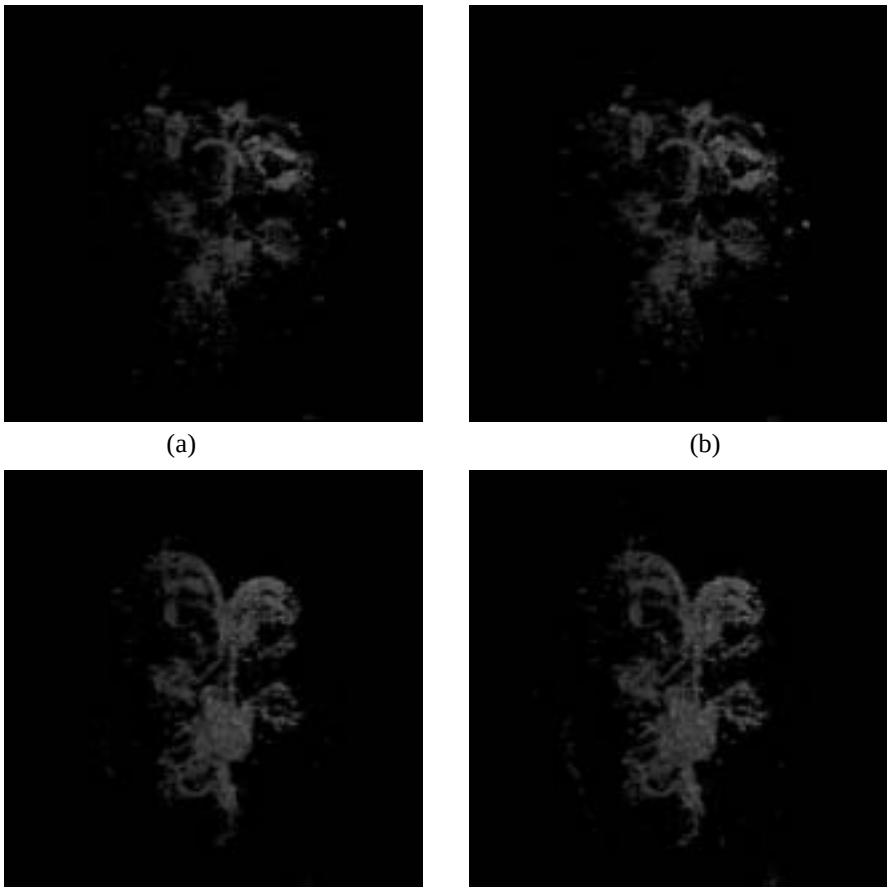

(a) (b)

(c) (d)

Figure 5: the volume rendering result after applying the first method of Wavelet transform. (a) a 3-level (b) a 4-level Wavelet transform for the first channel (c) a 3-level (d) a 4-level Wavelet transform for the second channel

Comparing Figure 4 and 5, it can be found that the fiber is indeed enhanced, backgrounds have been eliminated, but unwanted objects which cover neuron fiber still remained.

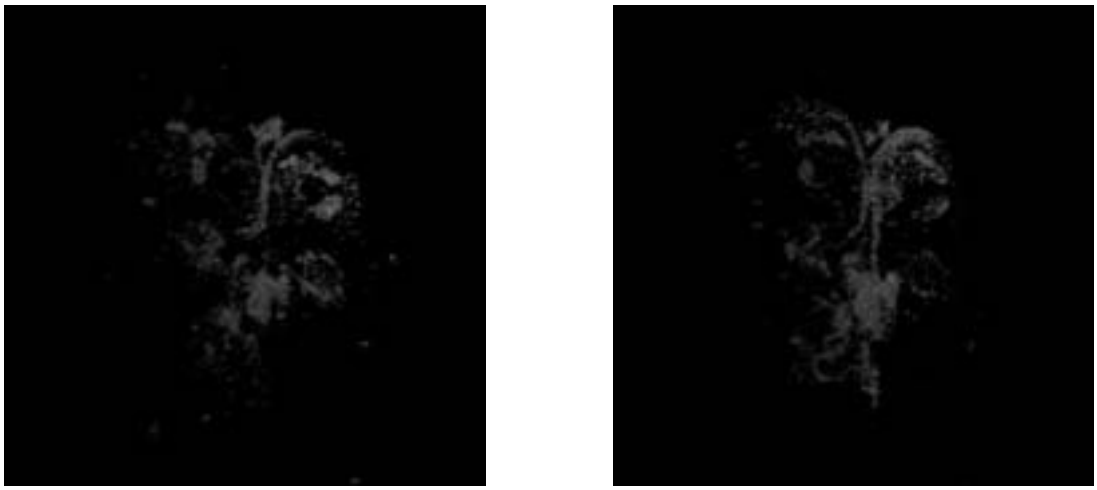

(a) (b)

Figure 6: the results after applying the second method of Wavelet transform (a) channel 1 and (b) channel 2

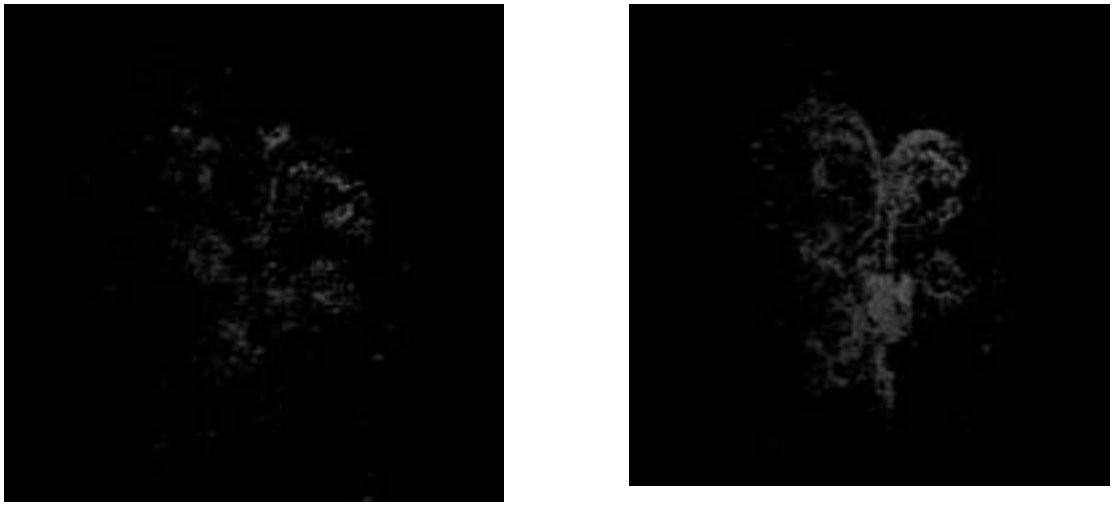

(a) (b)

Figure 7: The result obtained by applying Fourier Transform (a) the first channel, (b) the second channel

As shown in Figure 7, Fourier Transform is able to remove the background, but some of the desired objects are removed as well. The second method of Wavelet transform is better than the former one and Fourier transform.

4.2 RESULTS OBTAINED BY USING THE MATCHED FILTER

In this section, the results after applying the matched filter are presented. Figure 8 shows the result obtained by rendering the volume obtained by applying the matched filter to the original image. Figure 9 shows the result after first applying Fourier transform followed by the matched filter. Figure 10 shows the image obtained by applying a 3-level Wavelet transform followed by matched filter.

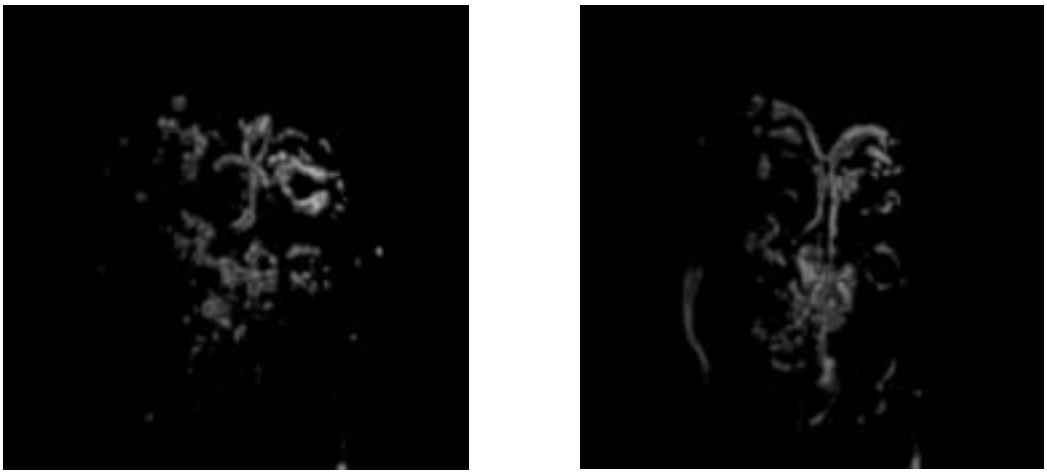

(a) (b)

Figure 8: results obtained by applying the matched filter to the original image (a) the first channel (b) the second channel

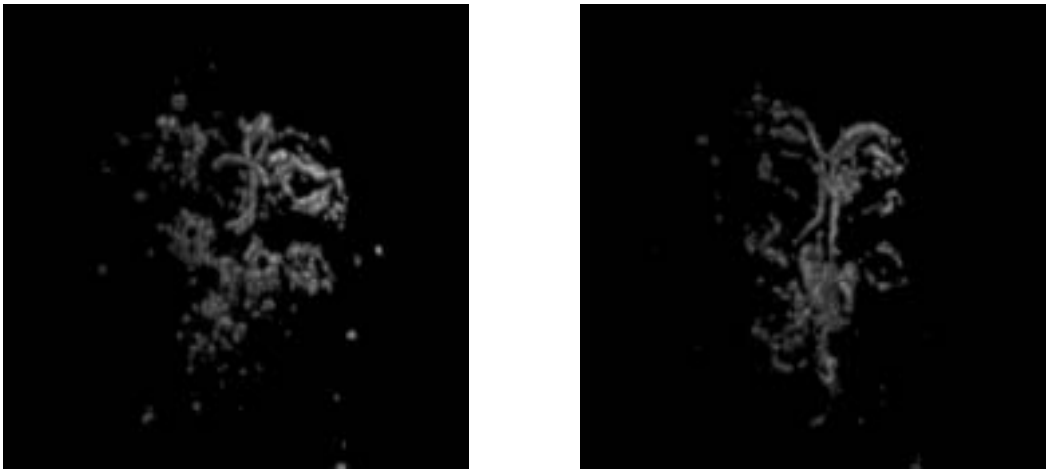

(a) (b)

Figure 9: results obtained by applying Fourier Transform image followed by matched filter (a) the first channel (b) the second channel.

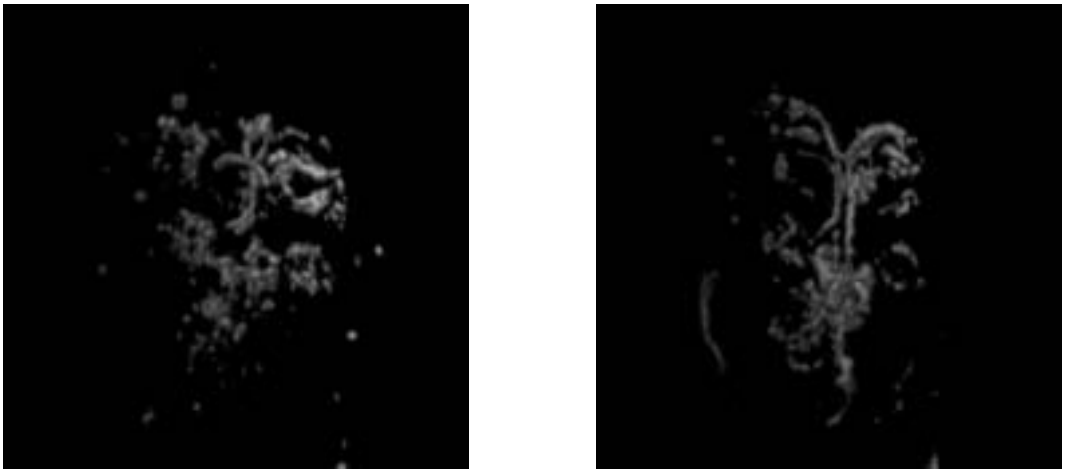

(a) (b)

Figure 10: results obtained by applying a 3-level Wavelet transform followed by the matched filter (a) the first channel (b) the second channel

Although Figure 8 and Figure 9 looks "cleaner" than Figure 10, but the image of Figure 10 is better than Figure 8 and Figure 9 due to the conservation of desired signals.

5. CONCLUSIONS AND SUMMARIES

In this study, we used the Wavelet transform to enhance the neuron fibers in confocal microscopic images. The first method of Wavelet transform is to multiply a constant *k* to *HH*, *HL*, and *LH* sub-images to enhance the high frequency components (the edge information are in the high frequency component). The second is to compute a new *LL* sub-image by subtracting the average of *LL* sub-images of two channels. Since the two channels have similarity backgrounds, this method works well to remove the common background. The second experiment is to apply the matched filter. In this experiment, the Wavelet transform follow by matched filter performed better than the other methods.

6. ACKNOWLEDGEMENTS

We thank to Professor A. S. Chiang, Department of Life Science, National Tsing Hua University, Hsinchu, Taiwan, for providing the data sets. This work was supported in part under the grant NSC-90-2213-E-009-119, National Science Council, Taiwan.

8. REFERENCES

1. Eric J. Stollnitz, Tony D. DeRose, and David H. Salesin, "Wavelets for Computer Graphics. Theory and Applications" Morgan Kaufmann Publishers, Inc., 1996.
2. Unser, Michael,1996."Wavelets, statistics, and biomedical applications," *8th IEEE Signal Processing Workshop on Statistical Signal and Array Processing*, Jun 1996 pp.: 244 -249
3. Anca Dima, Michale Scholz, and Klaus Obermayer, 2002. "Automatic Segmentation and Skeletonization of Neurons From Confocal Microscopy Images Based on the 3-D Wavelet Transform," *IEEE Transactions on Image Processing*, July, Vol. 11, NO. 7, pp. 790-801
4. Chih-Yang Lin, Yu-Tai Ching, S. James Chen, "Extraction of Coronary Arterial Tree Using Cine X-Ray Angiograms"
5. Khalid A. Al-Kofahi, Sharie Lasek, Donald H. Szarowski, Christopher J. Pace, and George Nagy, 2002. "Rapid Automated Three-Dimensional Tracing of Neurons From Confocal Image Stacks," IEEE Transactions on Information Technology in Biomedicine, June, Vol. 6, No. 2, pp. 171-187.
6. Chatterjee, S.; Chaudhuri, S.; Goldbaum, M.; Katz, N.; Nelson, M., 1989,"Detection of blood vessels in retinal images using two-dimensional matched filters," *IEEE Transactions on Medical Imaging*, Volume: 8 Issue: 3 , Sep 1989, pp. 263 -269
7. Goldbaum, M.; Hoover, A.D.; Kouznetsova, V., 2000, "Locating blood vessels in retinal images by piecewise threshold probing of a matched filter response," *IEEE Transactions on Medical Imaging,* Vol.: 19 Issue: 3 , Mar 2000, pp. 203 -210
8. S. Mallat, "A Theory fro Multiresolution Signal Decomposition: The Wavelet Representation," IEEE Trans.PAMI, vol. 11, pp. 647-693, 1999.
9. P. P. Vaidyanathan, "Multirate Systems And Filter Banks", Prentice Hall, Inc., 1993.
10. L. Cohen, "Time-Frequency Distributions - A Review," Proc. IEEE, Vol. 77, pp. 941-981, 1989